Journal of Power Sources 242 (2013) 106–113

Contents lists available at SciVerse ScienceDirect

Journal of Power Sources

journal homepage: www.elsevier.com/locate/jpowsour

Indirect fuel cell based on a redox-flow battery with a new design to avoid crossover

Zyun Siroma*, Shin-ichi Yamazaki, Naoko Fujiwara, Masafumi Asahi, Tsukasa Nagai, Tsutomu Ioroi

Research Institute for Ubiquitous Energy Devices, National Institute of Advanced Industrial Science and Technology (AIST), 1-8-31, Midorigaoka, Ikeda, Osaka 563-8577, Japan

HIGHLIGHTS

- A new structure for a redox flow battery to avoid crossover is proposed.
- An indirect fuel cell using the newly proposed redox flow battery was also proposed.
- The negative and positive halfs of an indirect fuel cell were demonstrated separately.

ARTICLE INFO

Article history:
Received 28 March 2013
Accepted 2 May 2013
Available online 25 May 2013

Keywords:
Redox flow battery
Proton-exchange membrane fuel cell
Indirect fuel cell
Carbon monoxide

ABSTRACT

A new design of a redox flow battery (RFB), which is composed of two subcells separated by a gas phase of hydrogen, is proposed to eliminate the crossover of ionic species between the anolyte and catholyte. This idea not only increases the possible combinations of the two electrolytes, but also opens up the prospect of a revival of the old idea of an indirect fuel cell, which is composed of an RFB and two chemical reactors to regenerate the electrolytes using a fuel and oxygen. This paper describes the operation of a subcell as a component of an indirect fuel cell system. In the cycling test, oxidation/reduction of the electroactive species in each electrolyte were repeated with a hydrogen electrode as the counter electrode. This result demonstrates the possibility of this newly proposed RFB without crossover. In the operation of the subcell with a chemical reactor, a molecular catalyst (a rhodium porphyrin) was dissolved in the anolyte, and then a fuel was bubbled in the anolyte reservoir. As the electroactive species was reduced by the fuel, a steady-state oxidation current was observed at the cell. This demonstrates the negative half of the newly proposed indirect fuel cell.

1. Introduction

A redox flow battery (RFB) is a secondary battery system composed of two tanks of two electrolytes, i.e., the anolyte and catholyte, each of which contains a soluble redox couple, and an electrochemical cell to generate electricity using the two electrolytes, which consists of two porous electrodes separated by an ion-exchange membrane [1,2]. Since this system has a unique characteristic that the magnitudes of the power and energy can be designed independently, it has been proposed as a major candidate for large-scale electricity storage systems. Based on RFB technology, the construction of an indirect fuel cell system in combination with two chemical reactors to regenerate the discharged anolyte and catholyte using a fuel and oxygen, respectively, has been proposed for several decades, as a “chemically regenerative redox fuel cell” or “redox fuel cell” [3–5]. The concept is schematically illustrated in Fig. 1. In the anolyte regenerator, the redox couple in the anolyte is reduced by the fuel with the help of a catalyst. In the catholyte regenerator, the redox couple in the catholyte is oxidized by oxygen with the help of another catalyst. The redox flow battery is operated using these two regenerated electrolytes. Overall, electric power is obtained from the fuel and oxygen. In this system, each redox couple in the anolyte and catholyte acts as a redox mediator which mediates electron transfer from the fuel to the anode, and from the cathode to oxygen, respectively. A “partly indirect fuel cell”, which uses a mediator for only the oxygen side [6] as an improved version of a proton-exchange membrane fuel cell (PEMFC), has also been proposed.

However, except the above-mentioned partly indirect fuel cell, there is a problem to be solved before an RFB can be used to

* Corresponding author.
E-mail address: siroma.z@aist.go.jp (Z. Siroma).

0378-7753/$ – see front matter © 2013 Elsevier B.V. All rights reserved.
http://dx.doi.org/10.1016/j.jpowsour.2013.05.061

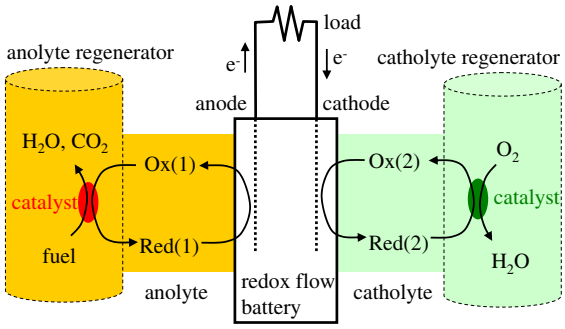

Fig. 1. Schematic of an indirect fuel cell.

construct an indirect fuel cell system. The anolyte and catholyte in an RFB are gradually mixed by diffusion through the electrolyte membrane [7]. Among the several types of RFBs that have been proposed and studied as energy storage systems [1,2], some are based on the concept of using a single element for both redox couples in the anolyte and catholyte, such as all-vanadium [8], all-chromium [9], and all-uranium [10]. This concept is an effective solution to the crossover problem, since mixing of the two electrolytes does not affect the components of the two electrolytes. Unfortunately, however, none of these RFBs can be used as a component of an indirect fuel cell system, because of the mismatch of the redox potentials. In an indirect fuel cell system, the potential of the redox mediator in the catholyte should be slightly lower than the open-circuit potential (OCP) of the oxygen electrode (ca. 1 V), while that in the anolyte should be slightly higher than the OCP of the hydrogen electrode (0 V). All-vanadium (or any other single element type) system does not satisfies this demand, and at this stage we have to use two different elements for redox mediators. This raises the crossover problem of mixing of two redox mediators, which represents irreversible deterioration of the system.

To help realize the commercial application of an indirect fuel cell, here we propose an RFB with a new design to avoid the crossover problem. Fig. 2 shows its concept in comparison with a conventional system. The new design incorporates negative and positive subcells connected in series. During a discharge process, the negative subcell combines oxidation of the anolyte at a porous electrode as an anode and the hydrogen evolution reaction (HER) at a gas diffusion electrode (GDE) as a cathode, whereas the positive subcell combines the hydrogen oxidation reaction (HOR) at a GDE as an anode and reduction of the catholyte at a porous electrode as a cathode. Since the anolyte and catholyte are separated by a gas phase of hydrogen, any species in the electrolytes, except water vapor, are blocked. As noted in Fig. 2(b), the cathode of the negative subcell, the anode of the positive subcell, the electric wire connecting them, and the gas phase of hydrogen act together as a proton-permselective membrane.

The two subcells in Fig. 2(b) have a common structure: a porous electrode for an electrolyte and a GDE for hydrogen. A half-cell can be tested independently with any electrolyte, regardless of whether it is intended to be use as an anolyte or catholyte in this system. This means that experiments to develop our new RFB are easier than those for a conventional RFB, in which reactions of the anolyte and catholyte can not be performed separately, and matching of the state-of-charges (SOC) of the two electrolytes should always be considered when interpreting the results. After we determine the performance of various electrolytes against hydrogen, we can estimate the performance of a hypothetical system constructed with a choice of any two electrolytes as the anolyte and catholyte.

The objective of this work was to examine the feasibility of two technologies which are essential for realizing our proposal of an indirect fuel cell system: the operation of a subcell of the new RFB,

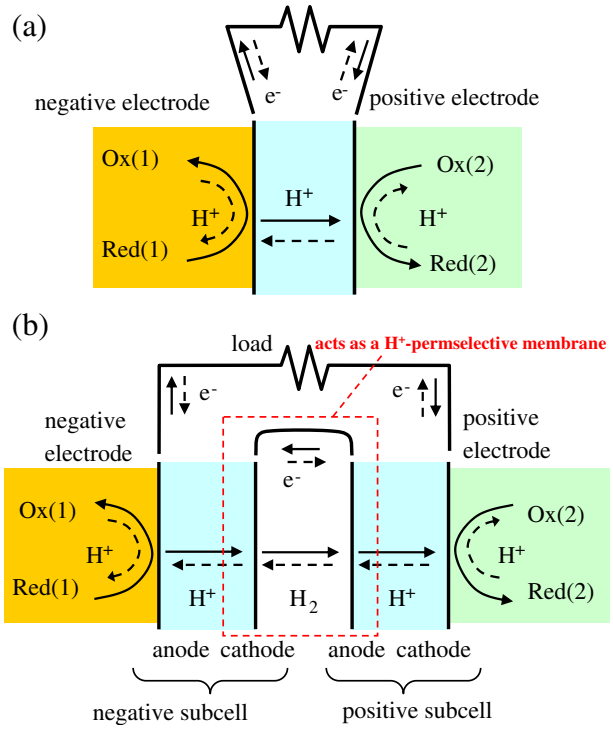

Fig. 2. Schematics of (a) conventional and (b) newly proposed RFBs. Dotted arrows represent inverse (charging) directions.

and the operation of a chemical reactor to regenerate the electrolyte. In the operation of a subcell, iron, indigocarmine, and an anthraquinone derivative were tested as electroactive species in the electrolytes. For each electrolyte, reduction/oxidation cycles of the electrolyte were performed against a hydrogen electrode. In the operation of a chemical reactor, an electrolyte containing an oxidized species was chemically reduced by carbon monoxide or hydrogen, with the aid of a rhodium porphyrin as a molecular catalyst. The steady-state operation of a subcell in combination with a chemical reactor was also tested.

2. Experimental

2.1. Subcell

A schematic illustration of the fabricated subcell is shown in Fig. 3. This represents a combination of PEMFC technology on the left half and RFB technology on the right half. The geometric active area of the electrodes was 2.25 cm^2. For the left side of the subcell, a unitized block with a casing and a flow field of H_2 was made of

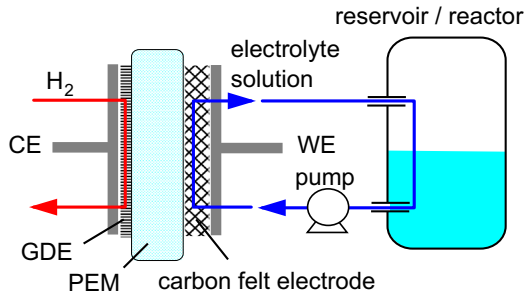

Fig. 3. Subcell consists of a gas diffusion electrode for hydrogen and a porous electrode for an electrolyte.

graphite. There is a channel to make a serpentine flow field with a width and depth of 1 mm each. For the right side of the subcell, a titanium plate as the current collector was embedded in a casing made of PTFE. While there is no flow channel, there is a space with a thickness of 1 mm for the electrode. Therefore, the electrolyte was penetrated through the carbon felt electrode described later. A membrane-electrode assembly (MEA) was made of a piece of PFSI membrane (Nafion® 117, DuPont) and a piece (1.5 cm-square) of commercially available electrode sheet for PEMFCs made from a Pt-catalyzed carbon black and a carbon cloth (ELAT, 0.5 mg-Pt cm^{-2}, E-TEK) by hot-pressing at 130 °C for 2 min. This electrode was used on the left side for HER/HOR. For the right side, a piece (1.5 cm-square) of carbon felt (GF20-3F, Nippon Carbon) was used as a porous electrode for reduction/oxidation of the electrolyte. The cell was maintained at 40 °C. One hundred mL of the test solution was put in the reservoir maintained at 40 °C, and circulated between the right side of the subcell by a pump (model 204, FLOM) with a flow rate of 10 mL min^{-1}. Fully humidified H_2 gas was fed at 10 ccm to the left side of the subcell. Except in experiments that used a reactant gas (fuel or oxygen), the atmosphere in the reservoir was kept inert by bubbling of N_2 with a flow rate of 20 mL min^{-1}. All data were collected using an electrochemical analyzer (636B, ALS).

2.2. Electrolyte solutions

An anthraquinone solution and an indigocarmine solution were used as potential candidates for the anolyte, and a ferric/ferrous electrolyte was used as a potential candidate for the catholyte. As the indigocarmine solution, 0.01 M indigocarmine (Tokyo Chemical Industry) in 0.5 M H_2SO_4 was prepared (abbreviated "IC electrolyte"). As the anthraquinone solution, 0.05 M disodium anthraquinone-2,6-disulfonate (Tokyo Chemical Industry) in 0.5 M H_2SO_4 was prepared (abbreviated "AQDS electrolyte"). A disulfonated anthraquinone was used to secure solubility. As the ferric/ferrous electrolyte, 0.1 M Fe^{3+} in 1 M HCl was prepared (abbreviated "iron electrolyte") from $FeCl_3 \cdot 6H_2O$ (Kishida Chemical). All of the reagents were of chemical grade and used without further purification. Due to the solubility limit, the concentration of the IC electrolyte was low, and its theoretical capacity is only one-fifth of those of the other two electrolytes. Before being used in the subcell, each electrolyte was characterized by CV in a beaker cell with a three-electrode configuration at 40 °C under an inert atmosphere of N_2 flow. A glassy carbon rod electrode (φ 3 mm, BAS), a Ag|AgCl|KCl(sat.) electrode (RE-1C, BAS), and a Pt wire were used as the working electrode, reference electrode, and counter electrode, respectively.

2.3. Catalysts and chemical reactor

As chemical catalysts to reduce the anolyte by fuels, solid or molecular catalysts were used. As the solid catalyst, a Pt black-plated Pt mesh (geometric area: 10 cm^2, φ 80 μm, 80 mesh, NILACO) was used. The electrochemical surface area (ECSA) was determined by CV in a 0.5 M H_2SO_4 solution just before use. A rhodium porphyrin was reported to catalyze the reduction of indigocarmine using CO as a reductant [11]. Furthermore, a rhodium carbonyl complex was reported to catalyze electrochemical oxidation of hydrogen [12]. In this work, as the molecular catalysts, 5,10,15,20-tetrakis(4-sulfophynyl)porphinato rhodium (III) (abbreviated "Rh-TPPS") and tetracarbonyldi-μ-chlorodirhodium (I) (Wako, abbreviated "Rh-CO") were used for CO and H_2 oxidation, respectively. Rh-TPPS was obtained by the reflux of $Rh_2Cl_2(CO)_4$ and 5,10,15,20-tetrakis(4-sulfophenyl)porphine in water (m/z 344, $[Rh^{III}(TPPS)]^{3-}$). The concentration of Rh-TPPS was calculated from the extinction coefficient of Rh tetracarboxyphenylporphine [13]. As a chemical catalyst to oxidize the catholyte by O_2, again, the Pt black-plated Pt mesh described above was used. To demonstrate the principle of the newly proposed indirect fuel cell, a catalyst was placed in the electrolyte reservoir of the subcell, and a reactant gas (H_2, CO or O_2) was bubbled at a flow rate of 100 mL min^{-1}. During this process, the reservoir acted as a chemical reactor to regenerate the electrolyte of the subcell.

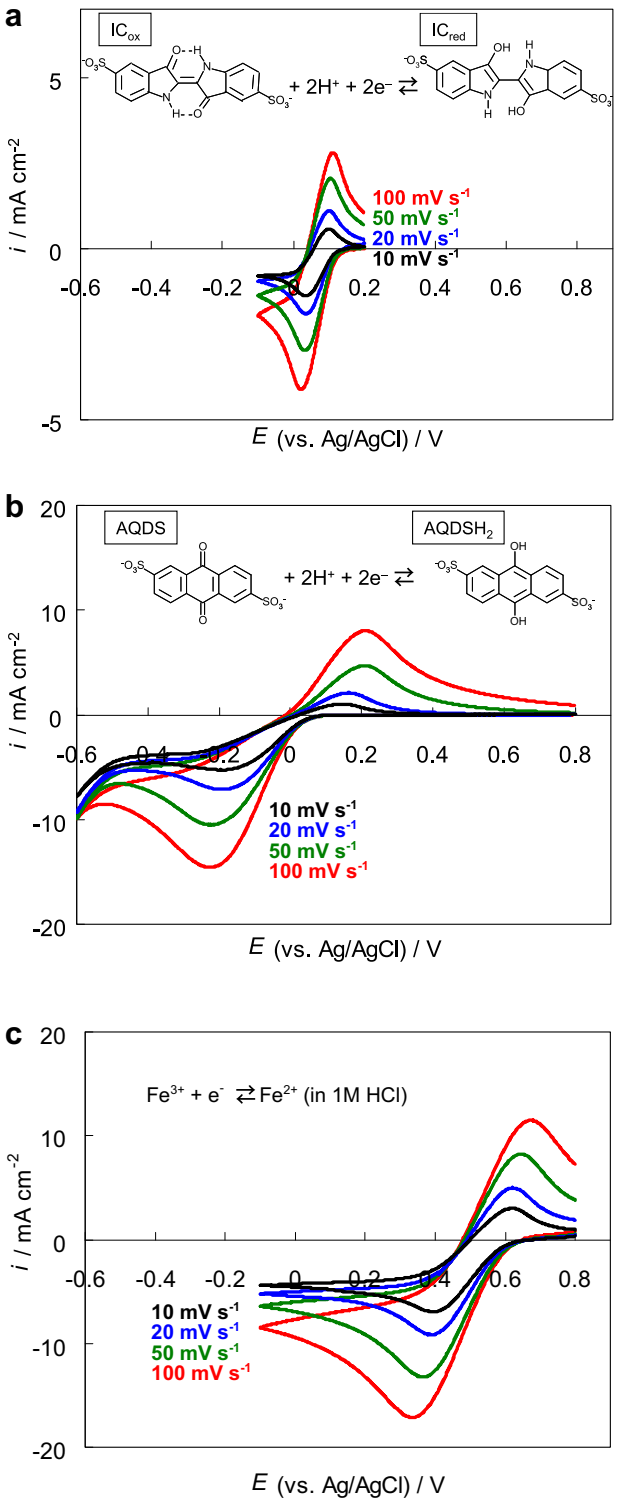

Fig. 4. CVs of (a) IC, (b) AQDS, and (c) iron electrolytes in a beaker cell with a three-electrode configuration.

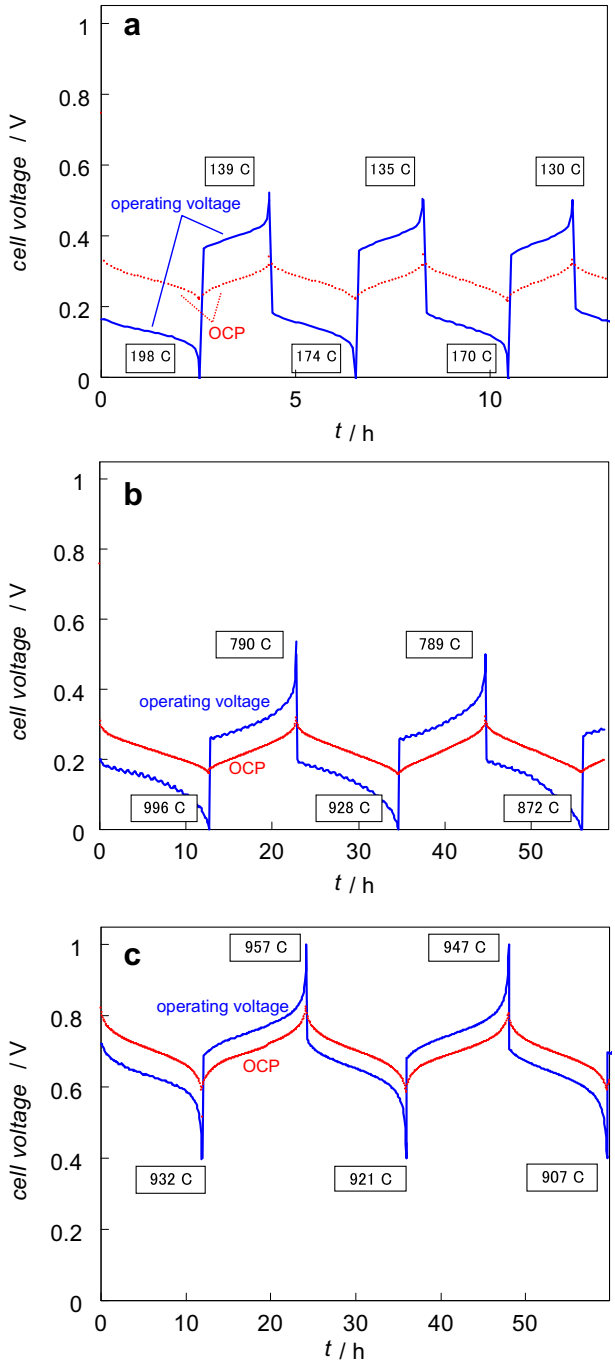

Fig. 5. Reduction/oxidation cycles of (a) IC, (b) AQDS, and (c) iron electrolytes. Thick blue lines and dotted red lines indicate operating voltage and open-circuit potential measured intermittently during operation, respectively. The capacities during each reduction/oxidation process are noted in a rectangle. The theoretical capacities of the three electrolytes are 193 C, 965 C, and 965 C, respectively. (For interpretation of the references to color in this figure legend, the reader is referred to the web version of this article.)

3. Results

3.1. Cycles of electrolytes

The results of a preliminary investigation of each electrolyte by CV in a beaker cell are shown in Fig. 4. The midpotentials obtained for the IC and AQDS electrolytes at 10 mV s^{-1} were 0.067 V and −0.024 V vs. Ag|AgCl, respectively. Although the results indicate that both electrolytes have similar equilibrium potentials of ca. 0.2∼0.3 V vs. RHE, a higher reversibility is suggested for the IC electrolyte. However, since the concentration is low, the peak currents for the IC electrolyte are lower than those for AQDS. The iron electrolyte showed a midpotential of 0.503 V vs. Ag|AgCl. Fig. 5 shows the first several reduction/oxidation cycles for each electrolyte against a hydrogen electrode as a counter electrode using the subcell. The current was set at 22.5 mA, which corresponds to 10 mA cm^{-2}. To monitor the redox condition of the electrolyte, the cell was kept in open-circuit conditions for 10 s intermittently every 300 s. The cell voltage measured during this off-time is also shown as OCP in the figures. The theoretical capacities of the IC and AQDS electrolytes were 193 C and 965 C, respectively, assuming two-electron reactions. The experimental value obtained in each reduction/oxidation process is noted in the figure, which is near the theoretical value. The slightly larger values during the reduction processes seem to be attributable to some side reaction such as HER. During the first oxidation process, the OCP values measured at the midpoint (SOC = 0.5) for the IC and AQDS electrolytes are 0.271 V and 0.225 V, respectively. The lower potential for the AQDS electrolyte is consistent with the preliminary results of CV.

At this stage, the performance of a hypothetical RFB using a pair of any two electrolytes can be estimated numerically. Fig. 6(a) shows a numerical estimation of the RFB system shown in Fig. 2(b) with a combination of the AQDS electrolyte as the anolyte and the iron electrolyte as the catholyte. This figure was made with one reduction/oxidation cycle of the AQDS electrolyte, and one

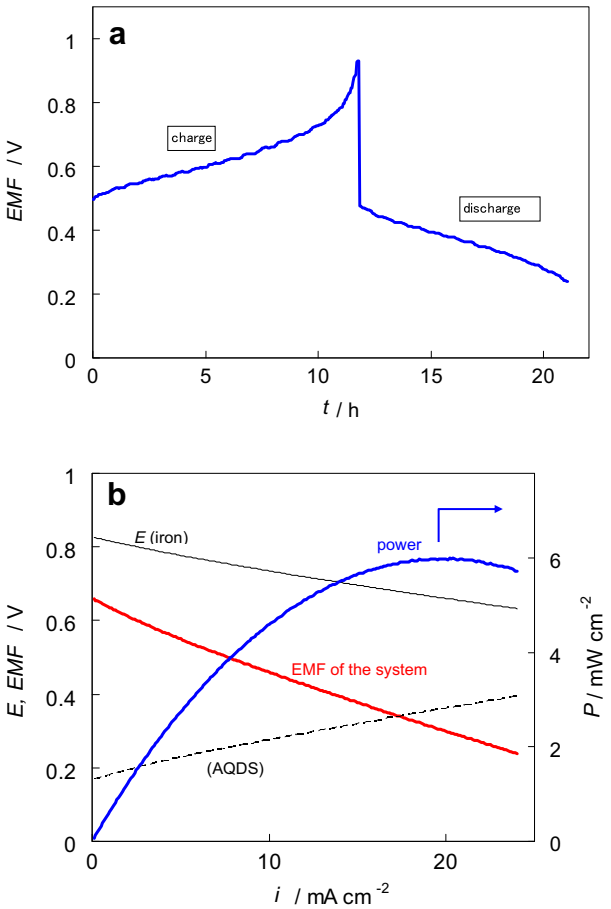

Fig. 6. Calculated expected (a) charge/discharge performance and (b) *I–V* performance in the fully charged condition for an RFB system that consists of AQDS and iron electrolytes.

oxidation/reduction cycle of the iron electrolyte. The average cell voltages during the charge and discharge processes are 0.63 V and 0.36 V, respectively. Based on the *I–V* characteristics of the subcell using each of the two electrolytes, the expected *I–V* characteristics of the total system can also be calculated, as shown in Fig. 6(b). This figure shows the oxidation performance of the AQDS electrolyte in the fully reduced condition, reduction performance of the iron electrolyte at the fully oxidized condition, and their difference.

3.2. Electrochemical oxidation of the IC electrolyte following chemical reduction

To confirm the principle of our new system, we started by examining the operation of the subcell shown in Fig. 3 with a Pt metal catalyst in the reservoir. Fig. 7(a) shows indirect H_2 oxidation using the IC electrolyte as a redox mediator with and without a Pt metal catalyst. The subcell just after an oxidation process of the cycling experiment was used, and the IC electrolyte was almost fully oxidized with an OCP of 0.315 V. Therefore, the cell voltage was set constant at 0.315 V for this experiment to start with no current. The bubbling gas was changed from N_2 to H_2 after starting the operation, which brought about a current rise. The expected reaction scheme is shown in Fig. 8. At the beginning, IC is almost fully oxidized state. As a fuel gas is introduced, the amount of the reduced state of IC increases and the redox potential of the electrolyte decreases. This change induces an oxidation current observed at the electrode of the cell. Even without the catalyst, a steady-state current of 5.6 mA (2.5 mA cm^{-2}) was observed, as shown as blank data in Fig. 7(a). This current was due to the chemical reaction of IC with H_2 oxidation, which proceeds even without the catalyst, and/or the direct electrochemical oxidation of dissolved H_2 at the electrode. The details of the assignment of this current in the blank condition will be discussed later for the case of AQDS. On the other hand, a steady-state current of 36.6 mA (16.3 mA cm^{-2}) was attained with the Pt catalyst. The difference between these two values is attributed to the catalytic activity of Pt. Fig. 7(b) shows indirect CO oxidation with and without the Rh-TPPS catalyst. In this case, no current was observed when the catalyst was absent. This means that CO hardly reacts with the IC electrolyte without a catalyst. Although a significant current was obtained with the catalyst, the value did not reach a steady sate in the time range of this experiment (120 min).

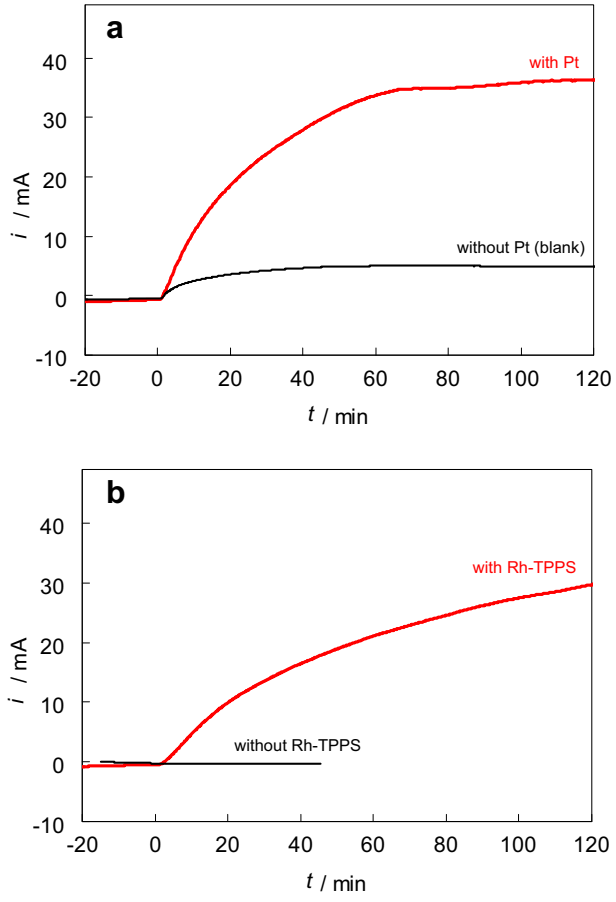

Fig. 7. Time courses of the electrochemical oxidation of the IC electrolyte using a subcell set at 0.315 V, simultaneously with reduction (a) by H_2 with a platinum black-plated platinum mesh (ECSA = 186 cm^2), and (b) by CO (10%, diluted by N_2) with the Rh-TPPS catalyst (0.14 mM) in the reservoir. Bubbling of the fuel gas in the reservoir was started at $t = 0$.

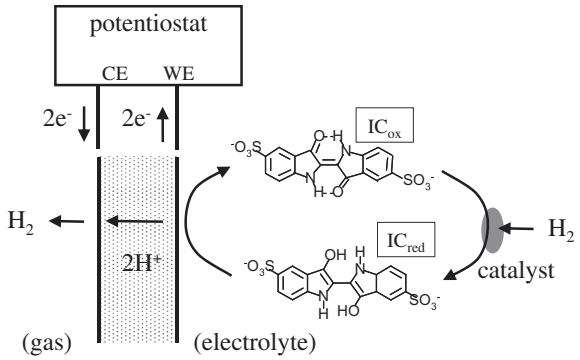

Fig. 8. Expected reaction scheme of the indirect H_2 oxidation shown in Fig. 7(a).

To eliminate the direct electrochemical oxidation at the electrode, the chemical reduction of IC by H_2 was also performed without simultaneous electrochemical oxidation. Each line in Fig. 9 shows changes in the OCP of the IC electrolyte by H_2 bubbling with the Pt catalyst without the production of electric current at the subcell. Equivalent electric charges that correspond to the amount of chemical reduction can be estimated using the relation between the electric charge and OCP derived from a discharge curve in Fig. 5(a), and are proportional to the duration of the bubbling in this time range. Based on this relation, the rate of the chemical reduction by H_2 in the reservoir was found to correspond to 59 mA. Since the electrolyte is under an almost fully oxidized state, this is an initial value and is higher than the steady-state value of 36.6 mA seen in Fig. 7(a). In Fig. 7(a), the OCP measured just after the

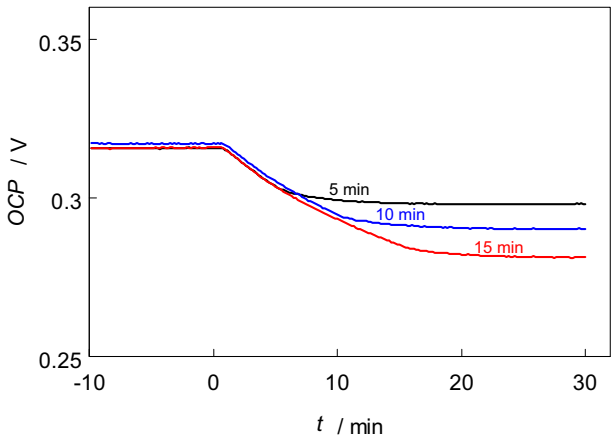

Fig. 9. Changes in the OCP of the IC electrolyte by H_2 bubbling for 5, 10, and 15 min in the presence of a platinum catalyst. H_2 bubbling was started at $t = 0$. N_2 bubbling was started just after H_2 bubbling was finished to purge H_2.

experiment was finished was 0.255 V, which is near the lower limit for this electrolyte. This suggests that the chemical reduction is fast and electrochemical oxidation determines the total rate under the steady-state condition in this case. Under the assumption that the electrolyte is fully reduced under the steady-state condition seen in Fig. 7(a), the time constant for approaching a steady-state condition can be roughly estimated as the ratio of the capacity of the electrolyte to the initial rate of the chemical reduction, i.e.,

$$193\ \mathrm{C}/59\ \mathrm{mA} = 55\ \mathrm{min} \quad (1)$$

This estimation is in fairly good agreement with the transient behavior seen in Fig. 7(a).

3.3. Electrochemical oxidation of the AQDS electrolyte following chemical reduction

Fig. 10 shows current values of indirect H_2 oxidation using the AQDS electrolyte as a redox mediator with and without the Rh-CO catalyst after reaching a steady-state condition plotted against the cell voltage. In these experiments, again, the electrochemical oxidation at the cell seems to be rate-determining. This estimation is supported by the fact that all data points are near the LSV result that was obtained with a fully reduced electrolyte, as shown by a dotted line. In contrast, only a small current was observed without the catalyst. The difference indicates the function of the catalyst. Furthermore, most of this small current can be attributed to the chemical reaction without the catalyst, but not direct electrochemical oxidation of the dissolved H_2, based on the fact that a much smaller current was observed without the mediator (H_2SO_4 only).

To demonstrate the possibility of using water gas as a fuel for an indirect fuel cell system, the indirect oxidation of a mixture of H_2 and CO using the AQDS electrolyte was performed with both Rh-CO and Rh-TPPS catalysts. Fig. 11(a) shows the electrochemical oxidation current along with chemical reduction, measured in the same manner as in Fig. 7. Since the capacity of the AQDS electrolyte is large (965 C), the observed current did not reach a steady-state condition in this time range. Therefore, instead of measuring a steady-state oxidation current, the reaction rates of the chemical reduction were estimated from changes in OCP during chemical reduction without electrochemical oxidation, in the same manner as in Fig. 9. The results and calculated equivalent currents that

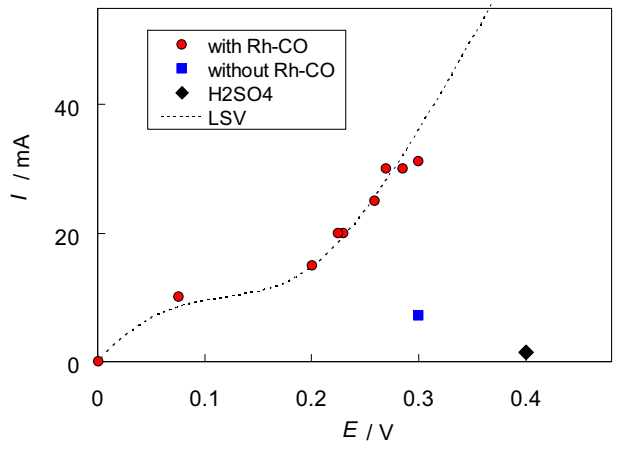

Fig. 10. Steady-state indirect oxidation of H_2 using the AQDS electrolyte with the Rh-CO catalyst (1 mM). Chronoamperometry or chronopotentiometry was performed until a steady-state was reached. The results with only 0.5 M H_2SO_4 as the electrolyte are also shown to estimate the magnitude of the direct oxidation of dissolved H_2 at the electrode. A dotted line shows the result of linear sweep voltammetry (5 mV s^{-1}) of the electrolyte under a fully reduced condition with saturated H_2 (OCP = 0.00 V).

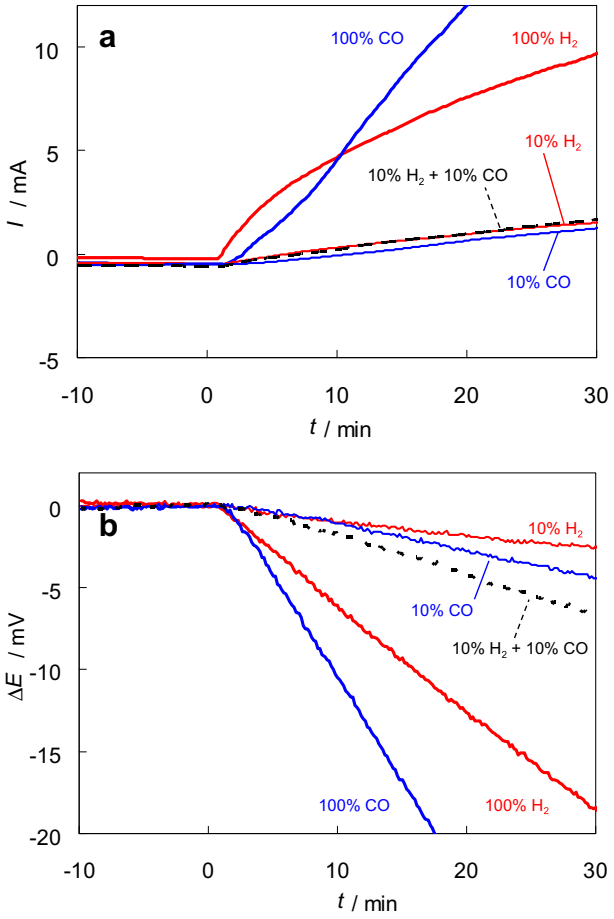

Fig. 11. Time courses of (a) the electrochemical oxidation of the AQDS electrolyte using the subcell set at 0.3 V simultaneously with reduction by CO and/or H_2 in the electrolyte reservoir, and (b) the decrease in OCP by chemical reduction without electrochemical oxidation. Fuel gas bubbling in the reservoir was started at $t = 0$. The Rh-CO catalyst (0.178 mM) and Rh-TPPS catalyst (1.05 mM) were added.

correspond to the chemical reduction rates are summarized in Fig. 11(b) and Table 1, respectively. Although the current is not strictly proportional to the concentrations of H_2 or CO, additivity is suggested from the results with a mixture of H_2 and CO. This means that reduction of the redox mediator by H_2 and CO proceeds independently. Compared with the simple results shown in Fig. 11(b), the behaviors of the current changes shown in Fig. 11(a) suggest rather complicated reaction rates. This is probably due to the effect of CO on the HER at the counter electrode, since a Pt catalyst was used for this reaction in this study.

3.4. Electrochemical reduction of the iron electrolyte following chemical oxidation

As a demonstration of the oxygen side of the indirect fuel cell, Fig. 12 shows indirect oxygen reduction using the iron electrolyte as

Table 1
Rates of chemical reduction of fuel gases estimated from the changes in OCP shown in Fig. 10(b).

Fuel gas	Equivalent current/mA
H_2 (100%)	53.1
CO (100%)	98.4
H_2 (10%) + N_2 (90%)	7.2
CO (10%) + N_2 (90%)	12.7
H_2 (10%) + CO (10%) + N_2 (80%)	19.3

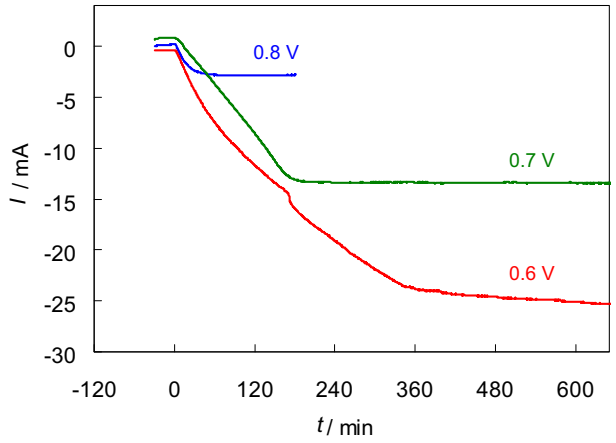

Fig. 12. Time courses of the electrochemical reduction of the iron electrolyte (in 0.5 M H_2SO_4) using the subcell set at 0.8, 0.7, and 0.6 V, simultaneously with oxidation by O_2 in the reservoir. O_2 bubbling was started at $t = 0$. A platinum black-plated platinum mesh (ECSA = 138 cm^2) was used as the catalyst in the reservoir.

a redox mediator with a Pt metal catalyst in the reservoir of the subcell. The voltage of the subcell was set at 0.8, 0.7, and 0.6 V. Before each experiment was started, the redox potential of the iron electrolyte was adjusted to be the same as the operating voltage. Since the iron electrolyte just after each experiment was finished was fully oxidized (with an OCP of higher than 0.8 V), electrochemical reduction also seemed to be rate-determining in this condition.

4. Discussion

4.1. Significance of indirect fuel cells

The important advantage of an indirect fuel cell is that it can use more and varied catalysts to oxidize the fuel and to reduce oxygen compared to direct-type fuel cells. In a direct-type fuel cell, a fuel or oxygen is involved in an electrochemical reaction, which, in principle, proceeds two-dimensionally, i.e., at the boundary between an ionically conducting phase and an electronically conducting phase. Therefore, mass-transfer of the reactant always hinders the reaction. Indeed, there have been technical attempts to enlarge the apparent thickness of the electrode by making quasi-three-dimensional phase boundaries [14,15]. However, even in such an electrode, the reaction rate is governed by the trade-off between the two mass-transfers, those of the ions and fuel at the anode and those of the ions and oxygen at the cathode [16–18]. Therefore, there is a limit in coping with the insufficient activity by thickening of the catalyst layer, which results in a practical limit of the apparent thickness of the catalyst layer. On the other hand, in an indirect fuel cell, a fuel or oxygen is involved in a chemical reaction, which proceeds three-dimensionally in a reactor. This means that mass-transfer does not limit the reaction rate. This is a great advantage, especially when using a catalyst that does not have sufficient activity. Since the reaction rate is expected to be proportional to the amount of catalyst, a low-activity catalyst can be managed simply by increasing the concentration or enlarging the reactor volume. In addition, an indirect fuel cell system should increase the types of catalyst that are applicable, since a catalyst without electronic conductivity, or a molecular catalyst in a dissolved state, can be used.

One of the main problems to be solved before the commercialization of PEMFCs is the need for a large amount of platinum for the cathode catalyst. Therefore, many studies have been performed on the development of non-platinum catalysts for the oxygen reduction reaction (ORR), including oxides [19] and carbonaceous material [20]. However, the development of such materials is still in progress, and they still have not achieved sufficient activity. On the other hand, such insufficient catalysts may be quite acceptable for use as the catalyst in a chemical reactor to regenerate the catholyte in an indirect fuel cell system. This situation is similar to that for the anode catalyst of a fuel cell that uses a fuel other than hydrogen. The development of direct-type fuel cells, such as a direct methanol fuel cell (DMFC), should overcome the insufficient power density that originates from low-activity of the anode catalyst [21]. This problem may also be addressed by adopting an indirect system, i.e., by changing the catalyst from a two-dimensional electrocatalyst to a three-dimensional chemical catalyst. Furthermore, even if the fuel of a PEMFC is hydrogen, the coexistence of a trace amount of carbon monoxide can significantly reduce the performance through the poisoning of platinum-based catalysts [22–24]. In addition, this problem becomes more complicated in an actual cell with non-uniform CO poisoning [24]. Since CO is barely oxidized, the CO concentration becomes higher at the outlet than the inlet, and downstream poisoning is more serious. Therefore, a CO-selective oxidation reactor is indispensable for a PEMFC system that uses a reformed gas from fossil fuels. This complicates the balance of plant (BOP), and prevents fuel cell vehicles (FCV) from being fueled by fossil fuels except for pure hydrogen. An indirect fuel cell system without a CO-selective oxidation reactor, or even a shift reactor, could be realized if a chemical reactor can be made to regenerate the anolyte through the oxidation of both hydrogen and CO.

Another advantage of an indirect fuel cell is the flexibility of its operation. If various kinds of fuels are planned to be used, only the reactor for the anolyte should be changed, and the rest can be shared. Furthermore, since the system contains an RFB, it can store electric energy when necessary. This means that the reaction rates at the two chemical reactors for the anolyte and catholyte do not have to always be synchronized with the output current. Therefore, while the size of the electrochemical cell should be secured in accordance with the instantaneous maximum output demand, the sizes of the two reactors can be reduced in accordance with the average output.

Due to these above-mentioned features, we believe that the development of an indirect fuel cell system supplied with a variety of fuels will become a key technology for overcoming the disadvantages of direct-type fuel cells such as a DMFC. Such a system could be used as a distributed power system in a community using biomass-originated fuels, such as water gas, alcohols, and sugars. Since the system can store energy, it could also be used to help moderate the fluctuating electricity generated from solar and wind. This system may also have an automotive application. The practical application of an indirect fuel cell that uses some liquid fuel such as methanol, or at least reformed gas made from some fossil fuel, should increase the cruising range of FCVs. Furthermore, since the system is inherently capable of storing electricity, additional secondary batteries can be omitted, which are usually required for an FCV to capture regenerative braking energy.

4.2. Significance of the new design of RFB

As described in the Introduction, here we propose a new design shown in Fig. 2(b) to separate the anolyte and catholyte. We believe that the realization of RFBs with this new design has independent value in the field of RFB as a device for energy storage. This design not only solves the crossover problem but also broadens the choice of the anolyte, catholyte, and their combination. For example, we can use a combination of a hydrochloric acid and a sulfuric acid, or

even an acid and an alkaline. It will encourage the reconsideration of possible active species.

The main disadvantage of this design is that overpotentials of the two additional reactions, i.e., HER and HOR, reduce the total EMF of the battery. However, these hydrogen reactions in general are known to be very fast, so this disadvantage can be minimized.

4.3. Challenges to realize indirect fuel cells

In this work, the steady-state operations of both indirect fuel oxidation in combination with HER and indirect ORR in combination with HOR were demonstrated using the subcell. This demonstrates the feasibility of constructing an indirect fuel cell system based on the new RFB with a hydrogen phase. Some technical problems will arise when two subcells are combined to construct a system, such as management of the pressure of the hydrogen phase between the two subcells, or balancing of the SOCs of the two electrolytes. These are subjects for a future study. Fortunately, the system has two electrodes at which HER can proceed. Therefore, an imbalance of the two SOCs can be redressed by choosing an electrode for excessive HER, which will be required to compensate dissipated hydrogen.

Our results showed that the rate-determining step of our cell is electrochemical reaction at the electrode, for both indirect fuel oxidation and indirect oxygen reduction. This is mainly due to inferior activity of the electrode, which can be speculated based on the large overpotentials observed in Fig. 5. Thus, the chemical reactor has a much greater activity than the electrochemical cell. From a practical viewpoint, proper allocation of the total voltage loss to each process is necessary. Improvement of the performance of the subcell is the most important task at this stage.

One of the main objectives is to eliminate the use of platinum catalysts in state-of-the-art PEMFCs. However, for the cathode side, only a platinum catalyst was tested in this work. The use of some non-platinum catalyst, such as has been reported for an indirect ORR system [6], on the cathode side of the indirect fuel cell system is required. Furthermore, a commercially available electrode with a platinum catalyst was used for the counter electrode (GDE for HER/HOR). Even though further reduction of the amount of platinum might be possible for this hydrogen electrode, it would be even more desirable to completely eliminate platinum from the system. The use of non-platinum HOR [25] and HER catalysts [26] should also be considered. As catalysts for the oxidation of fuels, it would also be preferable to eliminate noble metals, as well as platinum. We recently found a cobalt complex that could catalyze CO oxidation and mediator reduction [27]. Performance of this catalyst in our subcell is now under investigation.

5. Conclusion

A new structure for an RFB was proposed. The characteristic of the design is the use of a gas phase of hydrogen which acts as a proton-permselective membrane, and which solves the crossover problem. Based on this new RFB, an indirect fuel cell system was also proposed. A subcell, which is a common structure for the negative and positive halfs of an indirect fuel cell system, was made. Reduction/oxidation cycle tests of some electrolytes were performed using the subcell. The results demonstrated the feasibility of using the new RFB as a device for energy storage. Next, a catalyst for fuel oxidation or oxygen reduction was introduced in the electrolyte, which changed the electrolyte reservoir into a chemical reactor. Transient behaviors and steady-state operations were examined with both a fuel and oxygen. The results demonstrated the feasibility of this new indirect fuel cell system.

Acknowledgments

This work was supported by “Advanced Low Carbon Technology Research and Development Program” (ALCA), JST, Japan. The authors thank Dr. Sahori Takeda for the ESI-MS measurement to determine the Rh-porphyrine, and Ms. Yoshiko Murai for her help with the experimental set-up and data collection.

References

[1] A.Z. Weber, M.M. Mench, J.P. Meyers, P.N. Ross, J.T. Gostick, Q. Liu, J. Appl. Electrochem. 41 (2011) 1137–1164.
[2] M. Skyllas-Kazacos, M.H. Chakrabarti, S.A. Hajimolana, F.S. Mjalli, M. Saleem, J. Electrochem. Soc. 158 (2011) R55–R79.
[3] A.M. Posner, Fuel 34 (1955) 330–338.
[4] S. Ashimura, Y. Miyake, Denki Kagaku 31 (1963) 598–604.
[5] D.-G. Oei, J. Appl. Electrochem. 12 (1982) 41–51.
[6] A. Creeth, Fuel Cells Bull. 2011 (4) (2011) 12–15.
[7] Y.-W.D. Chen, K.S.V. Santhanam, A.J. Bard, J. Electrochem. Soc. 128 (1981) 1460–1467.
[8] M. Skyllas-Kazacos, M. Rychcik, R.G. Robins, A.G. Fane, M.A. Green, J. Electrochem. Soc. 133 (1986) 1057–1058.
[9] C.-H. Bae, E.P.L. Roberts, R.A.W. Dryfe, Electrochim. Acta 48 (2002) 279–287.
[10] T. Yamamura, Y. Shiokawa, H. Yamana, H. Moriyama, Electrochim. Acta 48 (2002) 43–50.
[11] J.C. Biffinger, S. Uppaluri, H. Sun, S.G. DiMagno, ACS Catal. 1 (2011) 764–771.
[12] J. Uribe-Godínez, R. Hernández-Castellanos, O. Jiménez-Sandoval, J. Power Sources 195 (2010) 7243–7245.
[13] S. Yamazaki, Y. Yamada, S. Takeda, M. Goto, T. Ioroi, Z. Siroma, K. Yasuda, Phys. Chem. Chem. Phys. 12 (2010) 8968–8976.
[14] E.A. Ticianelli, C.R. Derouin, A. Redondo, S. Srinivasan, J. Electrochem. Soc. 135 (1988) 2209–2214.
[15] Z. Poltarzewski, P. Staiti, V. Alderucci, W. Wieczorek, N. Giordano, J. Electrochem. Soc. 139 (1992) 761–765.
[16] Z. Siroma, T. Sasakura, K. Yasuda, M. Azuma, Y. Miyazaki, J. Electroanal. Chem. 546 (2003) 73–78.
[17] Y.G. Chirkov, V.I. Rostkin, Russ. J. Electrochem. 45 (2009) 183–191.
[18] Z. Siroma, K. Yasuda, Electrochemistry 79 (2011) 326–328.
[19] K. Lee, A. Ishihara, S. Mitsushima, N. Kamiya, K. Ota, Electrochim. Acta 49 (2004) 3479–3485.
[20] J. Ozaki, S. Tanifuji, N. Kimura, A. Furuichi, A. Oya, Carbon 44 (2006) 1324–1326.
[21] H. Liu, C. Song, L. Zhang, J. Zhang, H. Wang, D.P. Wilkinson, J. Power Sources 155 (2006) 95–110.
[22] J.-H. Wee, K.-Y. Lee, J. Power Sources 157 (2006) 128–135.
[23] G. Bender, M. Angelo, K. Bethune, R. Rocheleau, J. Power Sources 228 (2013) 159–169.
[24] C. Bonnet, L. Franck-Lacaze, S. Ronasi, S. Besse, F. Lapicque, Chem. Eng. Sci. 65 (2010) 3050–3058.
[25] A. Serov, C. Kwak, Appl. Catal. B 90 (2009) 313–320.
[26] J. Maruyama, T. Ioroi, Z. Siroma, T. Hasegawa, M. Mineshige, ChemCatChem 5 (2013) 130–133.
[27] S. Yamazaki, Z. Siroma, M. Yao, N. Fujiwara, M. Asahi, T. Ioroi, J. Power Sources 235 (2013) 105–110.